AUTOMATUM DATA:
Drone-based highway dataset for the development and validation of automated driving software for research and commercial applications

Paul Spannaus[1,2] Peter Zechel[1] Kilian Lenz[1]

***Abstract*— Recent innovation in highly automated driving in industrial and scientific domains has created a growing demand for logical description of statistically meaningful real-world motion data. On one hand this data supports learning-based probabilistic methods in software development while on the other it allows validation and testing.**

The *AUTOMATUM DATA* dataset is a new dataset which is now available at `automatum-data.com`, and was generated initially using 12 characteristic highway-like scenes from 30 hours of drone videos. The processing pipeline for determining the object trajectories was validated with reference vehicles, where the relative speed error was less than 0.2 percent. To generate the dataset described in this study, the objects from the drone videos were first identified and classified. The detected objects were then linked to their coordinate system results to produce valid object trajectories. The presented dataset is freely available for future research and development-based endeavors (Creative Commons license model CC BY-ND).

I. INTRODUCTION

The recent technological advances in functional features of highly automated driving is transforming the fundamental paradigm of automotive software development from a fully deterministic system to having a more probabilistic approach. The probabilistic approach allows more precise prediction of the probabilities of occurrence of other road users, their behavior, and allows smoother handling of complex maneuvers. The validation and development of such probability-based functions require a significant amount of representative observation-based data.The quantity and variance of these probability-based functions are dependant on extremely elaborate and cost-intensive test campaigns.

Safeguarding these complex vehicle functions requires testing efforts to be conducted in virtual format [41], [1], [39]. Cloud approaches support the scaling and scope of virtual safeguarding. In context of the release of safety-critical software, situation description validation in the real world is pertinent. Effective utilization of real driving behavior for virtual test drives is pertinent for successful commercialization and launch of the these highly automated driving functions.

Currently the various methods being used to generate the reference data include: test vehicles with highly accurate sensors, permanently installed measuring stations or aerial recordings acquired by drones providing bird's-eye view (top view). This study reports reference data generation using drones, as it has numerous advantages over the other methods in context of quality-based criteria.

The object-related motion of traffic can be derived from top-view images recorded by drones based on the quality criteria which includes: effective representation of natural behavior; precise description of scenes and boundary conditions; accurate dynamic object description; efficient data generation in highly variant traffic situations [5]. In this study, we developed two additional criteria which aim to improve the existing uncertainty of accuracy of the world coordinate system, and improve the static world representation of the scene.

With this publication, the first reference dataset of *AUTOMATUM DATA* has been presented, which was based on a wide array of top-view drone videos captured in highway-like traffic situations. In this context, the processing tool chain was designed in such a way that a continuous optimizations could be applied to all drone data recorded up to that point. Thus, new findings in data processing can potentially retroactively update the database. In this process, the pipeline of data processing was also used to validate the trajectory calculation in the world coordinate system by comparing the extracted object trajectories against the reference measurement system (inertial measurement unit) of the test vehicles. This study presents the current state of development of the tool chain simultaneously providing access to the most current fully-automated processed data. The available data consist of 12 characteristic highway-like scenes from 30 hours of drone videos which will be freely available to the scientific community and for potential commercial applications. Therefore, the dataset presented in this study is being published under the Creative Commons license CC BY-ND.

II. PREVIOUS WORK AND STATE OF THE ART

An increasing number of deterministic, rule-based vehicle functions (typical of SAE Level 1 and 2) are being augmented by probabilistic state models [7], [8], [9]. As the comprehensive understanding of the inner representation of the neural networks increases [10], more driving-related tasks may be successfully performed using the learned models.

Recent data generation approaches are based on a variety of methods which involve use of experimental vehicles equipped with high-accuracy sensors such as radar, lidar, and 360° cameras [17], [14], [16]. These experimental vehicles record the video from a driver's perspective, capturing all vehicular

[1] Automatum, `contact@automatum-data.com`; Dataset available on `www.automatum-data.com`

[2] EFS, Joint Venture of AKKA Industry Consulting GmbH and CARIAD SE, `paul.spannaus@efs-auto.com`

environmental parameters accurately [37], [15]. However, in this case the biggest problem is overshadowing of the road users by other vehicles, making them inconspicuous to the experimental vehicle driver [19]. Also, the test vehicles equipped with sensors may incite a change in behavior of the drivers involved, which remains unaccounted for in these types of studies [2], [35].

Sensors permanently installed in infrastructures are also an established method of data collection [21]. Although, a large amount of data can be collected using these sensors, the data collected by them may be flawed since vehicles may be masked behind larger vehicles, such as trucks. Moreover, these sensors collect data from a single location [5]. Therefore, using a drone is considered to be more accurate since it provides an aerial view of the roads [2], [45]. These small flying machines can remain undetected from the driver's view since they can be positioned at height of several hundred meters above the road. Drones are relatively inexpensive and easy to use, allowing capture of arbitrary road scenes easier [5], [18], [12].

A number of aerial road view-based datasets exist. The first dataset is that of the *NGSIM* Drone [2], which was introduced in 2011 and till date used as a reference dataset for traffic flow-based research [3],[4], which involves the use of four scenes captured using synchronized cameras. The Stanford dataset [44] primarily captured the movement and dynamics of pedestrians across the university campus, with very less cars forming an integral part of the data.

As part of the collaborative *Pegasus* project [1], the *highD* [5] dataset was generated. This captured six different highway segments and has since been updated *inD* [12] with data from road intersections, as well as *roundD* [11] traffic circles.

Most freely available reference datasets lack information about the relative changes in environment. The datasets primarily consist of data from highways, individual inner-city thoroughfare (traffic circles [15], [11], [13], and road-intersections [14], [12]). The *openDD* presents Breuer with [13] an extensive dataset under Creative Commons CC BY-ND for roundabout situations.

Recently numerous individual projects are coming up which are focusing on capturing large, interconnected traffic-based observations. Two major projects in this category worth mentioning include the *pNEUMA* project which aims at capturing traffic data around the Athens city center using a swarm of drones to reconstruct object movements [45]. The I-24 MOTION [21] project involves a deployment of 400 cameras along a U.S. highway which surveys a 4 mile stretch of road. Some of the generated database has been provided under different licensing terms. Also, approaches to framework formation [8] show imminent need for standardization [7]. The existing reference datasets have specific limitations. For example, the *NGSIM* dataset is characterized by a number of highly fluctuating bounding boxes which poses a challenge in the accurate computation of object-based trajectory [3].

In the *highD* dataset, the quantification of the generated trajectories was derived using the pixel resolution of the acquired image, with had a dimension of 10cm x 10cm with respect to the altitude of flight of the drone [5].

In this study the *AUTOMATUM DATA* dataset has been validated using data from reference sensors placed in test vehicles. The accuracy of the velocity determination was found to be 0.2%. The dataset presented in this study is available freely for potential use in research and commercial applications. The static world has been represented in the OpenDRIVE XODR standard. The automated pipeline allows for a top-down approach providing a broad scaling capacity. Additionally, the Python package has also been provided for free access, usage, and visualising of data. The dataset presented in this study contains representative motorway situations from 30 hours of video footage captured using drones at 12 motorway locations based in Germany with a steady stream of traffic.

III. APPLICATION OF AERIAL VIEW-BASED DATASETS

The aerial view provides a general perspective of the relative state of objects above the ground. If this is mapped to a world coordinate system (Universal Transverse Mercator - UTM) and considering that the object in question is a point mass, it may be possible to predict the physics of the motion dynamics of the object.

Therefore, based on this reference database various other research fields can be supported as enlisted below.

1) Accurate occupancy mapping and whereabout probability estimations of road users will assist in dealing with uncertainty of situations and will increase the efficiency of risk assessment based on these collision probability calculations [23].

2) Efficient behavior prediction of individual objects such as pedestrians [24], and human drivers exiting a highway [25] or behavior of extreme drivers [27] will allow establishment of expected value for acceptable acceleration-based behavior [9], or lead to more accurate traffic-related overload predictions [28] and let movement probabilities of individual road users be inferred effectively [26].

3) Advanced models in traffic flow theory and traffic observation which will interpret the traffic scene and predict traffic evolution and macroscopic traffic dynamics [29], [30], [31] providing data of interaction between few road users [32] and its effect on traffic flow [3], [33], [34];
followed by the development of a more complex mixed traffic model which integrates data of automobiles and motorcycles, respectively [31].

4) Higher-level management of transportation infrastructure can be effectively performed using this type of reference dataset [35], which includes urban planning and traffic management, such as congestion detection and establishment of appropriate speed limits [36] or enforcing appropriate strategies for emergency vehicles [37].

5) Methods for safety verification of vehicle functions relying on scenario-based approaches [6]. Reconstructed scenes have been reported to be used for simulations [38] exemplary realized with CarMaker, SUMO [39], and CARLA [40]. Increased accuracy of traffic prediction will allow successful

extrapolation of that knowledge over an entire urban area [34]. As described by Schoener [41], the extensive datasets of real-world reference scenes necessary for validation cannot be generated by individual data collection initiatives and may only be realistically achieved by adopting crowd-sourcing strategies [41]. Neurohr et al. [7] describes the necessity of adopting these networked approaches for achieving a proof of system with the ultimate goal of establishing a homogeneous and functional safety process and guideline.

IV. PIPELINE IMPLEMENTATION

The calculation and generation of *AUTOMATUM DATA* datasets from aerial videos has been presented in figure 1. The starting point consists of footage captured by arbitrary drones with reasonable resolution and details of their captured frame rate, flight altitude, and viewing angle.

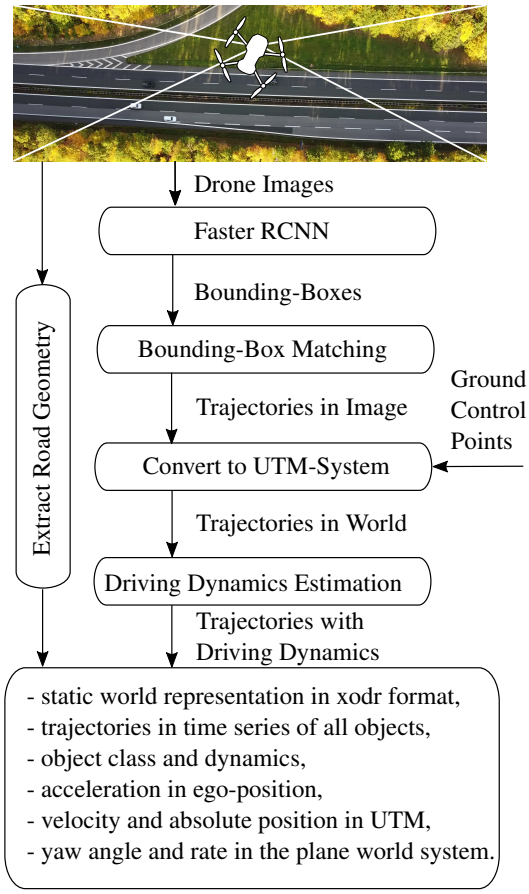

Fig. 1. Process and tooling chain for generating top-view reference datasets.

Each dataset $\mathcal{D}$ is defined as a set of images: $\mathcal{D} = \{\mathcal{I}_1, ...\mathcal{I}_k, ...\mathcal{I}_K\}$. Each image $\mathcal{I}_k^{H\times W\times 3}$ of a data set thus belongs to a defined time step $t_k = k \cdot f_{\text{sample}}^{-1}$ and has been acquired with resolution $H \times W$. Based on the recording time T and the sampling rate f_{sample} (frames per second - sample rate) of a data set $\mathcal{D}$, $k \in [0, K] \wedge k \in \mathbb{N}$ with $K = T \cdot f_{\text{sample}}$ holds.

A. Faster RCNN

In the first step Faster Region Based Convolutional Neural Networks *Faster-RCNN*, the position of the objects (in this case vehicles) in each image $\mathcal{I}_k$ of a dataset were detected. Since the data was processed after capture, there were no limitations on the computation time allowing application of computationally intensive yet effective artificial intelligence (AI)-based methods. According to [22], the Faster-RCNN network [46] is one of the most powerful networks for such applications. Thus, for each time step t_k, a set of detected bounding boxes $\mathcal{B}_k$ were calculated

$$\mathcal{B}_k = \{B_{1_k}, ...B_{n_k}, ...B_{N_k}\} = \text{Faster-RCNN}(\mathcal{I}_k), \quad (1)$$

where $N_k = |\mathcal{B}_k|$ describes the number of detected bounding boxes in the image $\mathcal{I}_k$. Correspondingly, the indexing of bounding boxes $n_k \in [0, N_k] \wedge n_k \in \mathbb{N}$. A bounding box B_{n_k} itself is defined as a tuple of two points (upper left and lower right corners): $B_{n_k} = \left([x_{\text{UL}}, y_{\text{UL}}]^T, [x_{\text{LR}}, y_{\text{LR}}]^T\right)$.

For case specific training of the pre-trained Faster RCNN, 1648 labels were generated in two-thirds of the recorded scenes. In the first step, the four vehicular classes consisting of *car, truck, carWithTrailer*, respectively were distinguished.

Of all the recorded videos 90 % were usable for subsequent data processing steps. Videos with involuntary drone movement caused by wind or light underexposure at the onset of dusk were unusable. In case of the dataset presented in this study a *DJI Mavic Mini* with 2K camera resolution was used.

B. Bounding-Box Matching

Based on the detected bounding boxes $\mathcal{B}_k$, the processing step *Bounding-Box Matching* now determines the trajectories distributed over time. For this purpose, all detected bounding boxes $\mathcal{B}_k$ belonging to an object i are required to be combined. From the reconstruction presented in this study, the trajectory $\mathcal{T}_i$ emerged as the set of bounding boxes B_{n_k}.

Each trajectory $\mathcal{T}_i$ has exactly one entry for each time frame in which the object is in the image, so that $|\mathcal{T}_i \cap \mathcal{B}_k| \leq 1$ holds ($|\mathcal{T}_i \cap \mathcal{B}_k| = 0$ when the object is no longer in the image, see Fig. 2.

The computation of $\mathcal{T}_i$ is currently performed based on the criterias of *distance* and *area overlap*, respectively. This part of the calculation is continuously evolving and retroactively improving the existing datasets. A computer vision based matching was, due the minor movements of objects within two frames, not necessary. Finally, this processing step resulted in I trajectories $\mathcal{T}_i$ with $i \in [0, I] \wedge i \in \mathbb{N}$.

C. Conversion of Trajectory to Universal Transverse Mercator (UTM) System

The conversion of the trajectories $\mathcal{T}_i$ from image coordinates to a metric world coordinate system (UTM [43]) was implemented in the data processing step *Convert to UTM-System*. For this purpose, the center image of the dataset was defined as the reference image $\mathcal{I}_{\text{ref}} = \mathcal{I}_{K/2}$. This reference image was based on typically 6 to 12 ground control points [42], with a homography matrix [48] $H^{3\times 3}$ being determined for the relevant UTM zone of the coordinate system. This

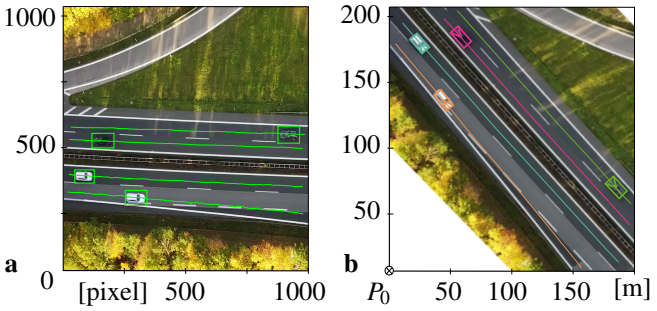

Fig. 2. All bounding boxes have been merged into trajectories.

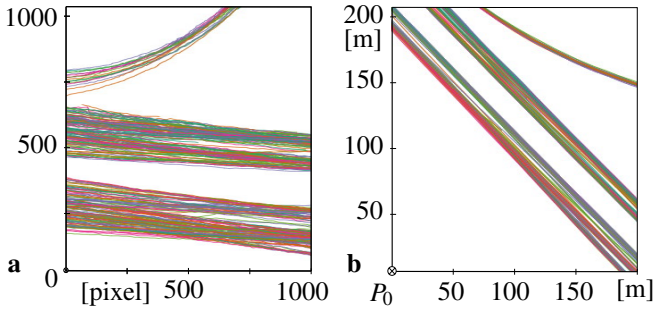

Fig. 4. Motion correction results in exact matching of trajectories with reference image $\mathcal{I}_{\text{ref}}$.

homography describes the transformation of the acquired image into a world coordinate system in the reference image. Thus, the bounding boxes $\mathcal{B}_k$ can be transformed into a metric coordinate system. This step allows to compensate for perspective and optical distortions caused by the camera or position of the drone, see Fig. 3.

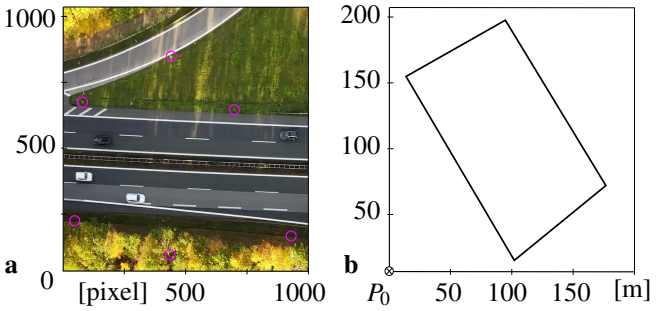

Fig. 3. The perspective distortions are determined by measured ground control points and compensated by the homography matrix.

D. Image Stabilization

Modern systems allow compensation against drone's motion and its flight turbulence, and the camera itself is usually well-stabilized with a gimbal controller. However, complete lack of deviations in image acquisition cannot be guaranteed.

Thus, the previously generated homography matrix $H^{3\times3}$ is only valid for the reference image $\mathcal{I}_{\text{ref}}$. For each image $\mathcal{I}_k$ a rotation and a translation correction to the reference image $\mathcal{I}_{\text{ref}}$ is necessary. These two corrections were mapped in the matrix $E_k^{2\times3}$ and this correction was based on a sparse feature set [48]. The conversion of point coordinates in an image (x, y) to metric coordinates in the current UTM zone results in Eq 2. and Eq. 3.

$$[x_{\text{imgStab}}, y_{\text{imgStab}}]^T = E_k \cdot [x, y, 1]^T \,, \tag{2}$$

$$P_{\text{UTM}} = H \cdot [x_{\text{imgStab}}, y_{\text{imgStab}}, 1]^T \,. \tag{3}$$

The correction and transformation of all trajectories have been shown in figure 4.

E. Estimation of the Driving Dynamics

The final step involved the *Estimation of the Driving Dynamics*. Thereby, the motion of the objects is derived from the determined bounding boxes. To remove uncertainties caused of the fluctuation of the bounding Boxes resulting from the image recognition process (Faster-RCNN) additional filtering is applied.

The signal processing method described by Loess and Jacoby [49] *locally-weighted scatterplot smoothing* (LOESS) was adopted for this study. This method implements a filtering method which corresponds to an iterative, local four-stage least square filtering method. These non-parametric regression method weighted the data point with the k-nearest neighbors [50] . The choice of the weighting window length is based on the maximum dynamics of the physical quantities position, velocity and acceleration. In this way, object-related system dynamics are taken into account. Therefore, it is not necessary for model-based filtering methods such as Kalman filtering.

This step results in the velocity v, the yaw angle ψ in the earth coordinate system as well as in the vehicle fixed accelerations (object coordinate system) in longitudinal a_x and lateral direction a_y. In combination with the manually extracted static world a logical representation of the entire traffic scene was created.

V. STRUCTURE OF THE DATABASE

Each video corresponds to an independent dataset, which on one hand consists of a static scene description in OpenDrive XODR format, while on the other consists of a JSON file with motion data of all the objects. Additionally, there is metadata, which contains basic information about the recording.

With the help of the metadata, the dataset can be filtered for the desired scene, road type, average length of the contained trajectories, weather, and location, as well as the version of the pipeline with which the video was processed. The latter may also be used for future recalculation for improving the data processing. The dataset can be visualized conveniently using a local-server-based visualisation as shown in Fig: 5. For the use and interfacing with the dataset, please refer to the project website, where the current interface descriptions have been published. For the most efficient handling of the dataset a utility library has been provided which consists of an object-oriented data structure that allows easy and efficient access to the respective datasets.

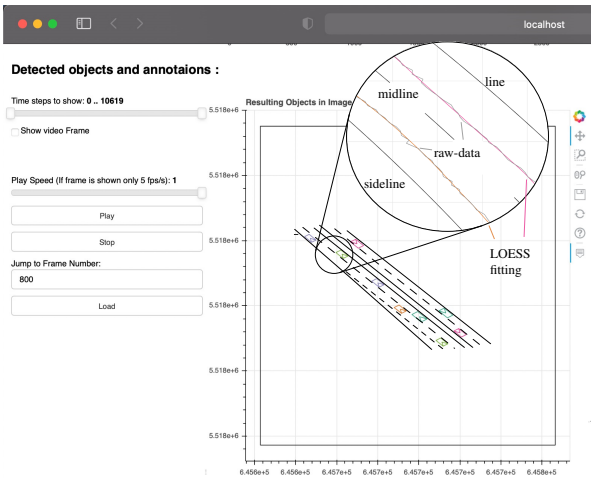

Fig. 5. A graphical Webserver application facilitates the review of data. The zoom showes the comparison between raw signal and LOESS filtering.

VI. VALIDATION OF DATA PROCESSING

In order to be able to make a statement about the quality of the data processing, it is pertinent to provide evidence of valid results being produced by the processing chain. For example, for the *highD* [5] dataset, the conversion of the pixel resolution to the physical distance per pixel of the area captured was presented.

For the validation of the processing chain presented in this study, test vehicles of an industrial partner were used to determine the error between the motion trajectories generated via the *AUTOMATUM DATA* tool chain and the reference measurement system. Figure 6 shows the two reference vehicles with inertial measurement units which were driving in column. Three measurements were run between two roundabouts. The data recording ran permanently in the vehicles and is therefore shown continuously in the plot. The vehicles went out of the drone capture zone several times, which lead to the recorded video capture only fragments of the test drive. Figure 7 shows the validity of the velocity profiles v

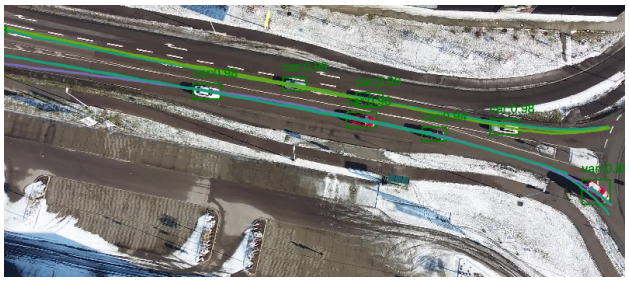

Fig. 6. Validation trajectories of two reference vehicles (red, white).

and the derived rotation of the objects in the world coordinate system $\dot{\psi}$, as well as the vehicular fixed accelerations a_x, a_y.

To quantify the deviation, the cross-correlation between vehicle reference measurement and drone database of the three measurement runs were performed (No.1, No.2, No.3):

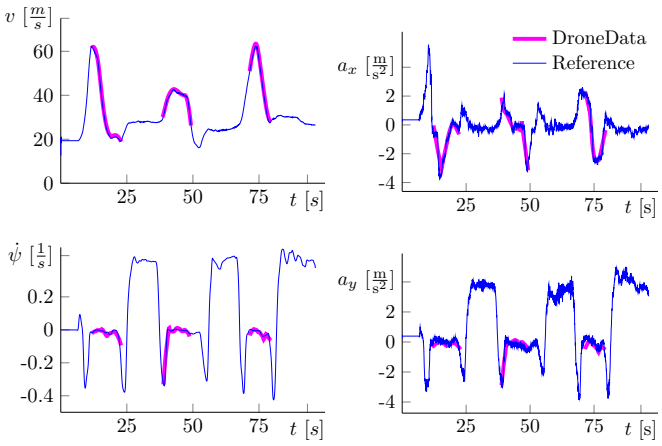

Fig. 7. Validation of the motion profiles extracted from the drones with the speed profile of the corresponding vehicle.

Relative Error	No.1	No.2	No.3
v	0.99987	0.99983	0.99996
a	0.97526	0.96958	0.98831
$\dot{\psi}$	0.86479	0.89263	0.86300

The largest deviation showed up in the determination of the yaw rate, since the deviation of longitudinal and lateral dynamics weighted over the tangent of their ratios. The relative error was less than 0.2 percent for results representing the positioning in the world coordinate system and the velocity-based calculations.

VII. CONCLUSION

The new dataset *AUTOMATUM DATA* is now available at `automatum-data.com`. This dataset includes 12 characteristic highway-like scenes from 30 hours of drone videos. Compared to previous datasets, a validation of the object trajectories was performed using a reference vehicle. The quality of the data processing pipeline presented in this study is reflected by the low velocity error of less than 0.2 percent as confirmed by the validation process. The data set was generated with the greatest care, however, deviations can possibly occur and the correctness could not be guaranteed.

This data processing pipeline allows generation of data from a wide range of drone videos for further research and development of highly automated vehicles. The publication of further datasets in different situations may be tackled in the future.

REFERENCES

[1] PEGASUS Research Project: Securing Automated Driving Effectively. (2020) Lectures and publications of the project. [Online]. Available: https://www.pegasusprojekt.de/de/lectures-publications.

[2] V. Punzo, M. T. Borzacchiello and B. Ciuffo. "On the assessment of vehicle trajectory data accuracy and application to the next generation simulation (ngsim) program data," *Transportation Research Part C Emerging Technologies*, vol. 19, pp. 1243–1262, 12 2011.

[3] B. Coifman, and L. Li. "A critical evaluation of the next generation simulation (ngsim) vehicle trajectory dataset," *Transportation Research Part B: Methodological*, vol. 105, pp. 362–377, 11 2017.

[4] D. Lovell. "Kinematics-enabled lossless compression of freeway and arterial vehicle trajectories," *Journal of Intelligent Transportation Systems*, vol. 23, pp. 1–25, 01 2019.

[5] R. Krajewski, J. Bock, L. Kloeker and L. Eckstein. "The highd dataset: A drone dataset of naturalistic vehicle trajectories on german highways for validation of highly automated driving systems," in *2018 21st International Conference on Intelligent Transportation Systems (ITSC)*, 2018, pp. 2118–2125.

[6] S. Riedmaier, T. Ponn, D. Ludwig, B. Schick and F. Diermeyer. "Survey on scenario-based safety assessment of automated vehicles," *IEEE Access*, vol. 8, pp. 87, 456–477, 2020.

[7] C. Neurohr, et al. "Criticality analysis for the verification and validation of automated vehicles," *IEEE Access*, 01 2021.

[8] F. Poggenhans, J. Pauls, J. Janosovits, et al. "Lanelet2: A high-definition map framework for the future of automated driving," in *2018 21st International Conference on Intelligent Transportation Systems (ITSC)*, 2018, pp. 1672–1679.

[9] D. Ridel *et al*. "A literature review on the prediction of pedestrian behavior in urban scenarios," in *2018 21st International Conference on Intelligent Transportation Systems (ITSC)*, 2018, pp. 3105–3112.

[10] K. Fabi and J. Schneider, "On feature relevance uncertainty: A monte carlo dropout sampling approach," on *arXiv: 2008.01468 [cs.LG]*, 2020.

[11] A. Breuer, *et al.* "opendd: A large-scale roundabout drone dataset," in *2020 IEEE 23rd International Conference on Intelligent Transportation Systems (ITSC)*, 2020, pp. 1–6.

[12] J. Bock, *et al*. "The ind dataset: A drone dataset of naturalistic road user trajectories at german intersections," in *2020 IEEE Intelligent Vehicles Symposium (IV)*, 2020, pp. 1929–1934.

[13] A. Breuer, *et al*. "openDD: A large-scale roundabout drone dataset," in *2020 IEEE 23rd International Conference on Intelligent Transportation Systems (ITSC)*, 2020, pp. 1–6.

[14] W. Zhan *et al*. "Constructing a highly interactive vehicle motion dataset," in *2019 IEEE/RSJ International Conference on Intelligent Robots and Systems (IROS)*, 2019, pp. 6415–6420.

[15] A. Zyner, S. Worrall, and E. Nebot. "ACFR Five Roundabouts Dataset: NaturalisticDriving at Unsignalised Intersections," in *IEEE Intelligent Transportation Systems Magazine*, 2019.

[16] A. Geiger, C. Stiller and R. Urtasun. "Vision meets robotics: The kitti-dataset," *International Journal of Robotics Research (IJRR)*, 2013.

[17] P. Sun, *et al*. "Scalability in perception for autonomous driving: Waymo open dataset," on *arXiv: 1912.04838v7 [cs.CV]*, 2019.

[18] D. Zhao and X. Li. "Real-world trajectory extraction from aerial videos - a comprehensive and effective solution," in *2019 IEEE Intelligent Transportation Systems Conference (ITSC)*, 2019, pp. 2854–2859.

[19] K. Messaoud, I. Yahiaoui, A. Verroust and F. Nashashibi. "Attention based vehicle trajectory prediction," *IEEE Transactions on Intelligent Vehicles*, vol. PP, 04 2020.

[20] A. Clausse, S. Benslimane and A. de La Fortelle. "Large-scale extraction of accurate vehicle trajectories for driving behavior learning," in *2019 IEEE Intelligent Vehicles Symposium (IV)*, 2019, pp. 2391–2396.

[21] D. Gloudemans, *et al*. "Interstate-24 motion: Closing the loop on smart mobility," in *2020 IEEE Workshop on Design Automation for CPS and IoT (DESTION)*, 2020, pp. 49–55.

[22] J. Huang, *et al*. "Speed/accuracy trade-offs for modern convolutional object detectors," in *Proceedings of the IEEE conference on computer vision and pattern recognition*, 2017, pp. 7310-7311.

[23] M. Khakzar, A. Rakotonirainy, A. Bond and S.G. Dehkordi. "A dual learning model for vehicle trajectory prediction," *IEEE Access*, vol. 8, pp. 21897–21908, 2020.

[24] P. Zechel, R. Streiter, K. Bogenberger and U. Göhner. "Pedestrian occupancy prediction for autonomous vehicles," in *2019 Third IEEE International Conference on Robotic Computing (IRC)*. IEEE, 2019, pp. 230–235.

[25] P. Zechel, R. Streiter, K. Bogenberger and U. Göhner. "Assumptions of lateral acceleration behavior limits for prediction tasks in autonomous vehicles," in *2019 7. International Conference on Mechatronics Engineering (ICOM)*, 2019, pp. 1–6.

[26] P. Zechel, R. Streiter, K. Bogenberger and U. Göhner. "Over-Approximation of the Driver Behavior as Occupancy Prediction," in *2019 IEEE 14th International Conference on Intelligent Systems and Knowledge Engineering (ISKE)*, 2019, pp. 735–742.

[27] K. Wang, Q. Xue, Y. Xing and C. Li. "Improve aggressive driver recognition using collision surrogate measurement and imbalanced class boosting," *International Journal of Environmental Research and Public Health*, vol. 17, p. 2375, 03 2020.

[28] A. Pierson, W. Schwarting, S. Karaman and D. Rus. "Learning risk level set parameters from data sets for safer driving," in *2019 IEEE Intelligent Vehicles Symposium (IV)*, 2019, pp. 273–280.

[29] R. Keane and H. Gao. "Calibration for traffic microsimulation using trajectory data: Fast calibration using the adjoint method," *CoRR*, 2019.

[30] L. Li, *et al*. "Trajectory data-based traffic flow studies: A revisit," *Transportation Research Part C Emerging Technologies*, vol. 114, 02 2020.

[31] A. Chen, *et al*. "Conflict analytics through the vehicle safety space in mixed traffic flows using uav image sequences," *Transportation Research Part C Emerging Technologies*, 10 2020.

[32] F. Diehl, T. Brunner, M. T. Le and A. Knoll. "Graph neural networks for modelling traffic participant interaction," in *2019 IEEE Intelligent Vehicles Symposium (IV)*, 2019, pp. 695–701.

[33] Y. Dülgar, M. Menth, H. Rehborn and M. Koller. "Analysis of microstructures in traffic jams on highways based on drone observations," in *2019 IEEE International Conference on Vehicular Electronics and Safety (ICVES)*, 2019, pp. 1–6.

[34] B. Yue, S. Shi, S. Wang and N. Lin. "Low-cost urban test scenario generation using microscopic traffic simulation," *IEEE Access*, vol. 8, pp. 123 398–123 407, 2020.

[35] F. Outay, H.A. Mengash and M. Adnan. "Applications of unmanned aerial vehicle (uav) in road safety, traffic and highway infrastructure management: Recent advances and challenges," *Transportation Research Part A: Policy and Practice*, vol. 141, pp. 116 – 129, 2020.

[36] M. Oliskevych, *et al*. "Optimization of vehicle speed forecasting horizont on the intercity highway," *Eastern-European Journal of Enterprise Technologies*, vol. 3, pp. 57–68, 06 2020.

[37] H. Rehborn, M. Koller and S. Kaufmann. "How traffic data are measured," in *Data-Driven Traffic Engineering*, Elsevier, 2021, pp. 5 – 28.

[38] S. Jesenski, J.E. Stellet, F. Schiegg and J.M. Zöllner. "Generation of scenes in intersections for the validation of highly automated driving functions," in *2019 IEEE Intelligent Vehicles Symposium (IV)*, 2019, pp. 502–509.

[39] F. A. Schiegg, J. Krost, S. Jesenski and J. Frye. "A novel simulation framework for the design and testing of advanced driver assistance systems," in *2019 IEEE 90th Vehicular Technology Conference (VTC2019-Fall)*, 2019, pp. 1–6.

[40] B. Osiński, *et al*. "Carla real traffic scenarios – novel training ground and benchmark for autonomous driving,"on *arXiv: 2012.11329 [cs.RO]*, 2020.

[41] H.P. Schoener. "Challenging highway scenarios beyond collision avoidance for autonomous vehicle certification," on *Researchgate preprint*, 11 2020.

[42] H. Ebner and T. Ohlhof. "Utilization of ground control points for image orientation without point identification in image space," in *ISPRS Commission III Symposium: Spatial Information from Digital Photogrammetry and Computer Vision*, vol. 2357, 1994, pp. 206–211.

[43] R.B. Langley. "The UTM grid system," *GPS world*, vol. 9, no. 2, pp. 46–50, 1998.

[44] A. Robicquet, A. Sadeghian, A. Alahi and S. Savarese. "Learning Social Etiquette: Human Trajectory Prediction In Crowded Scenes," in *European Conference on Computer Vision (ECCV)*, 2016.

[45] E. Barmpounakis and N. Geroliminis. "On the new era of urban traffic monitoring with massive drone data: The pNEUMA large-scale field experiment," *Transportation Research Part C: Emerging Technologies*, vol. 111, pp. 55–71, 2020.

[46] S. Ren, K. He and J. Sun. "Faster R-CNN: Towards Real-Time Object Detection with Region Proposal Networks," on *arXiv: 1506.01497v3 [cs.CV]*, 2016.

[47] H. Wang and Y. Liu. "Characteristic Line of Planar Homography Matrix and Its Applications in Camera Calibration," *18th International Conference on Pattern Recognition (ICPR'06)*, 2006, pp. 147-150.

[48] M. Tipping. "Sparse Bayesian Learning and the Relevance Vector Mach," *Journal of Machine Learning Research*, 2001, pp. 211–244.

[49] W. Jacoby and G. Loess. "A Ponparametric, Graphical Tool for Depicting Relationships Between Variables." In: *Electoral Studies*, 2000, no. 4, pp. 577–613.

[50] W. S. Cleveland. "Robust Locally Weighted Regression and Smoothing Scatterplots." In: *Journal of the American Statistical Association*, 1979, pp. 829–836.